scientific reports

Check for updates

OPEN

C/N ratio effect on oily wastewater treatment using column type SBR: machine learning prediction and metagenomics study

Nadeem A. Khan[1]✉, Abhradeep Majumder[2], Simranjeet Singh[3], Praveen C. Ramamurthy[3], Sandra Kathott Prakash[4], I. H. Farooqi[5], Nastaran Mozaffari[6], Dahiru U. Lawal[1,8] & Isam H. Aljundi[1,7]✉

The sequencing batch reactor has emerged as a promising technology in treating wastewater; however, its application in the treatment of generated water still needs to be explored. This research gap led to the investigation of various carbon-to-nitrogen (C/N) ratios in a column-type sequencing batch reactor (cSBR). The resulting data and model demonstrated that augmenting the SND process with an external carbon source is effective until the C/N ratio reaches 15, ultimately eliminating nitrogen in the produced water. Conversely, a reduced C/N ratio can limit the ability of polyphosphate-accumulating organisms to incorporate carbon into polyphosphate synthesis, thereby decreasing phosphorus removal efficiency within the cSBR. When the C/N ratio ranged from 6 to 8, and the mixed liquor suspended solids concentration was high, the average phosphate removal was approximately 55%, compared to only around 25% when the C/N ratio was less than 6.

Keywords Coastal wastewater, Sequencing batch reactor, Stress intensity, Artificial neural network, Interactive effect, Circular economy

Excess nutrients in aquatic systems, resulting from sewage discharge or industrial pollutants, can lead to eutrophication and acidification. In order to treat the excess nutrients, especially the nitrogen fraction of the wastewater, simultaneous nitrification and denitrification (SND) has emerged as a promising technology[1]. Both heterotrophic and autotrophic nitrifiers are essential in typical SND systems. Autotrophic nitrifiers, such as *Nitrosomonas* (ammonia-oxidizing bacteria) and *Nitrobacte*r (nitrite-oxidizing bacteria), have been found to consume a significant amount of alkalinity during oxidation of ammonia[2,3]. The nitrifiers thrive in situations with high levels of dissolved oxygen (DO), often above 1.0 mg/L, which is ideal for their growth. Heterotrophic nitrifiers, such as *Paracoccus* and *Thiosphaera*, are commonly found in habitats characterized by abundant organic carbon and low quantities of DO (less than 1.0 mg/L)[2,3]. In order to facilitate the cellular synthesis and proliferation of ammonia-oxidizing bacteria (AOB), a minimum carbonate alkalinity of 45 mg/L as $CaCO_3$ is necessary for nitrification, and a pH in the range of 7–8 is desirable[4,5]. These microorganisms govern denitrification and nitrification in the SND processes. These microorganisms possess the capacity to denitrify, aiding in maintaining the balance of alkalinity in SND systems, even if heterotrophic nitrification leads to a decrease in alkalinity[6,7].

The widespread industrialization demand for oil and natural goods necessitates a better understanding of the strain that produced water places on traditional treatment methods[8]. In recent years, sequencing batch reactors (SBRs) have advanced due to their robust nature and smaller footprint compared to conventional treatment

[1]Interdisciplinary Research Center for Membranes and Water Security (IRC-MWS), King Fahd University of Petroleum and Minerals, 31261 Dhahran, Saudi Arabia. [2]Department of Civil Engineering, Birla Institute of Technology and Science, Pilani Hyderabad Campus, Hyderabad 500078, India. [3]Interdisciplinary Centre for Water Research (ICWaR), Indian Institute of Science, Bangalore 560012, India. [4]Department of Biosciences and Bioengineering, Indian Institute of Technology, Roorkee, Uttarakhand, India. [5]Civil Engineering Department, Zakir Hussain College of Engineering and Technology, Aligarh Muslim University, Aligarh, India. [6]Chemical Engineering Department, Laval University, Quebec, QC, Canada. [7]Chemical Engineering Department, King Fahd University of Petroleum and Minerals, 31261 Dhahran, Saudi Arabia. [8]Mechanical Engineering Department, King Fahd University of Petroleum and Minerals, 31261 Dhahran, Saudi Arabia. ✉email: nadeem.khan@mecw.ac.in; aljundi@kfupm.edu.sa

methods. Wastewater now often contains varying amounts of recalcitrant compounds, making it more challenging to treat. Machine learning offers the potential to understand this complexity and develop efficient models for future predictions[9–11]. Past studies have prompted reevaluating strategies to enhance the overall SND process in column-type sequencing batch reactors (cSBRs). Establishing the optimal carbon-to-nitrogen (C/N) ratio values is crucial for improving the SND process in these reactors[12–16].

The development of more accurate and efficient treatment schemes will help reduce costs. This work introduces an aerobic cSBR to address the existing research gap in the treatment of produced water[17]. In the cSBR process, denitrifying organisms can be protected by influent organics, which can take the form of intracellular carbon during the initial anaerobic phase, aiding in nutrient removal during denitrification[18]. Over the past few decades, the focus has been on low C/N ratio wastewater for denitrification, often overlooking the rate-limiting step of nitrification. Nitrification, a well-established process in SBRs, is facilitated by nitrite-oxidising bacteria[19]. However, these bacteria' low production and high environmental vulnerability restrict their overall efficiency in nitrification[20]. Introducing an external carbon source that supports the SND process by converting ammonia to nitrogen can address the shortcomings of heterotrophic nitrification[21]. However, controlling the dosage of external carbon is challenging and relies on variables such as recirculation rate and DO content. Moreover, the utilization of external carbon sources leads to higher operational expenses and an increase in sludge generation[22]. Although the addition of external carbon sources may increase the cost of treatment in terms of procuring additional chemicals and also requiring regular monitoring since these carbon sources are required to be added in such a way that a desired C/N ratio is maintained, carbon is a vital electron donor for effective heterotrophic denitrification to take place[23,24]. External carbon enhances the performance of biological treatment systems by providing microorganisms with energy, hence accelerating the decrease of denitrification processes and chemical oxygen demand (COD). Microorganisms utilize carbon to catalyze the conversion of nitrates (NO^{3-}) into inert nitrogen gas (N_2) by denitrification, hence reducing total nitrogen (TN) levels in the treated effluent. This capability is crucial for complying with stringent nitrogen discharge limitations, which are more prevalent due to their significant environmental impact on the bodies of water where they are discharged[23–26]. Therefore, nitrification efficiency can be improved by incorporating heterotrophic nitrification into cSBR, which may require an additional carbon source that can be converted into intracellular carbon[27]. Heterotrophic nitrification not only aids the SND process but also leaves more energy available for other processes. In the past decade, it has been reported that heterotrophic nitrifying bacteria, such as *Acinetobacter, Thauera,* and *Pseudomonas,* possess phosphate-accumulating capabilities[17]. This suggests that intracellular carbon can transform during nitrification, contributing to the overall SND process. However, an insufficient carbon supply reduces nitrification, while an excess can inhibit the activity of endogenous functional microorganisms[17]. The presence of abundant organic carbon may favor the growth of heterotrophic bacteria over nitrifying bacteria. Heterotrophic bacteria, utilizing organic carbon, may outcompete nitrifiers for resources, decreasing nitrification rates[28].

The primary objective of the present study is to determine the efficiency of SND under varying operational parameters and to develop a biological mechanism for SND in column-type cSBRs by utilizing intracellular carbon sources as functional genes during the SND process. The results indicate that cSBRs supplemented with external carbon sources are highly effective in achieving a robust SND process. However, it was also observed that high C/N ratios inhibit both heterotrophic and autotrophic nitrifiers in produced water. The findings provide detailed insights into the interdependence between intracellular carbon and the SND process, suggesting a viable nitrogen removal pathway in the treatment of produced water. This work contributes to a deeper understanding of the role of external carbon sources in the SND process, potentially enhancing the efficiency of produced water treatment.

Material and methods

Sample collection and lab scale setup

A lab scale-column type SBR was established with a practical volume of 3.31 L, internal diameters of around 75mm, and a height of approximately 750 mm (Fig. 1). The reactor was inoculated with sludge from the nearby wastewater treatment plant aeration tank situated in Al Khobar (Dammam). The system was allowed to get acclimatized, after which the experimental trials were carried out. The temperature of the reactor's was retained at 25 ± 2 °C along with a surface aeration system to uphold 2–2.5 mg/L of DO throughout the operational run phase. The feeding and the decanting were controlled with the help of a PLC (program logic circuit) system operated at different time phases so that hydraulic retention time (eff. HRT) reached the optimum value of 53–13 h.

The volumetric exchange ratio was kept at 45%, increasing retention time to 21 h. The three ports at 25%, 50%, and 75% were also controlled using a PLC system, and mixed liquor suspended solid (MLSS) values were maintained at 3.2–3.5 g/L during the entire study thereby making solid retention time (SRT) of around 30–40 days. The grab samples from the 50% port were collected during the research and at different phase change intervals when the sludge settled down after the decanting phase. Diluted-produced water was fed to the reactor (initially 1 in 8, 1 in 6, 1 in 4, and 1 in 2) with different C/N ratios with municipal wastewater. External carbon sources such as starch and acetate, ammonium chloride as nitrogen sources, and dihydrogen potassium phosphate as phosphorus sources were used with micronutrients dissolved in distilled water. Earlier, researchers proposed that the carbon-to-nitrogen ratio directly influences the efficacy of nitrogen removal in constructed wetland systems[29]. Zhi and Ji noted that when the carbon-to-nitrogen ratio exceeded 6, there was no build-up of NO_2–N or NO_3–N, suggesting that denitrification was fully occurring[30]. Another study also observed that increasing the organic carbon source facilitated higher nitrogen removal[31]. Hence, the role of the C/N ratio in influencing the SND process has been explored in this work. The COD concentration in the rector was 450–550 mg/L, thereby maintaining the C/N ratio as 2, 6, 10, and 15, respectively. The sludge was taken at the end of each cycle to avoid the hypoxia effect that indirectly interfered with nitrification activity. The sludge underwent centrifugation for 5

Fig. 1. Lab-scale setup of column-type sequencing batch reactor.

min at a speed of 11,000 rpm. It was then rinsed two times with a solution of 0.9% sodium chloride and thereafter kept at a temperature 4 °C. As mentioned above, the anaerobic culture was kept in the dark phase for 2 h and rewashed. The autotropic nitrification activity deducts the values obtained for total ammonia oxidation activity with heterotrophic nitrification. The initial run was made with an eff. HRT of 53 h with a fill time of 0.26 h, react time of 52 h, settle time of 0.49 h, and decant time of 0.25 h. The eff. hydraulic retention time (HRT) was gradually lowered from 53 to 40 h (fill time of 0.26 h, React time of 39 h, settle time of 0.51 h, and Decant time of 0.23 h), 35 h (fill time of 0.26 h, React time of 34 h, settle time 0.51 h and decant time of 0.23 h), 22 h (fill time of 0.26 h, React time of 21 h, settle time 0.5 h and decant time of 0.24 h), 8 h (fill time of 0.26 h, React time of 17 h and settle time 0.5 h and decant time of 0.24 h) and finally 13 h (fill time of 0.26 h, React time of 12.5 h and settle time 0.08 h and decant time of 0.16 h). The samples were collected after each run during the different phases of operations. The experiments were conducted in triplicates to minimize experimental mistakes. Figure 2 displays the schematic diagram of the experimental setup.

Analytical methods

All the samples were tested in triplicate with COD, biochemical oxygen demand (BOD_5), MLSS, nitrate, phosphate, mixed liquor volatile suspended solids (MLVSS) measurements, and Sludge volume index SVI was measured using standard methods[32]. The measurement of COD was conducted using the comparative reflux method during each phase of the operation. The BOD was measured using a conventional setup of setting up different dilution bottles and measuring the DO[33]. The DO pH was measured using a Hach multiparameter fitted with probes (Hach, HQ30d). MLSS and MLVSS values were determined using the conventional method mentioned in the standard procedure [34]. The macronutrient used in the study has a composition in the ratio of $MgSO_4$: $CaCl_2$ as 20:1 and trace nutrients such as $FeCl_3{\cdot}6H_2O$, 0.1 $MnCl_2{\cdot}4H_2O$, 0.04 $CuSO_4{\cdot}5H_2O$, 0.2 H_3BO_3, 0.2 KI, 0.2 $CoCl_2{\cdot}6H_2O$, 0.2 $Na_2MoO_4{\cdot}2H_2O$, 0.3 $ZnSO_4{\cdot}7H_2O$, and 8 Ethylenediaminetetraacetic acid (EDTA); and 235 mg/L $NaHCO_3$ was used for alkalinity attainment. pH was adjusted to the neutral range using 2 M HCl. Table 1 shows the aerobic and nitrogen removal studies from various literature, whereas the table represents the TN in the cSBR at different C/N ratios (Table 2).

The intracellular carbon transformation efficiency of phosphate-accumulating and glycogen-accumulating organisms was estimated using Eq. 1.

$$E_C = \left(1 - \frac{(1.71(a_{in} - a_{anae}) + 2.86(b_{in} - b_{anae}))}{c_{in} - c_{anae}}\right) \times 100\% \quad (1)$$

It is understandable that heterotrophic systems initially take up the COD and lead to intracellular carbon using glycogen and phosphate accumulating organisms. where a (nitrite conc. in influent tank) = NO_2^-–N, b (nitrate conc. in influent tank) = NO_3–N, subffix in is for influent , anab. For different phases, c = COD.

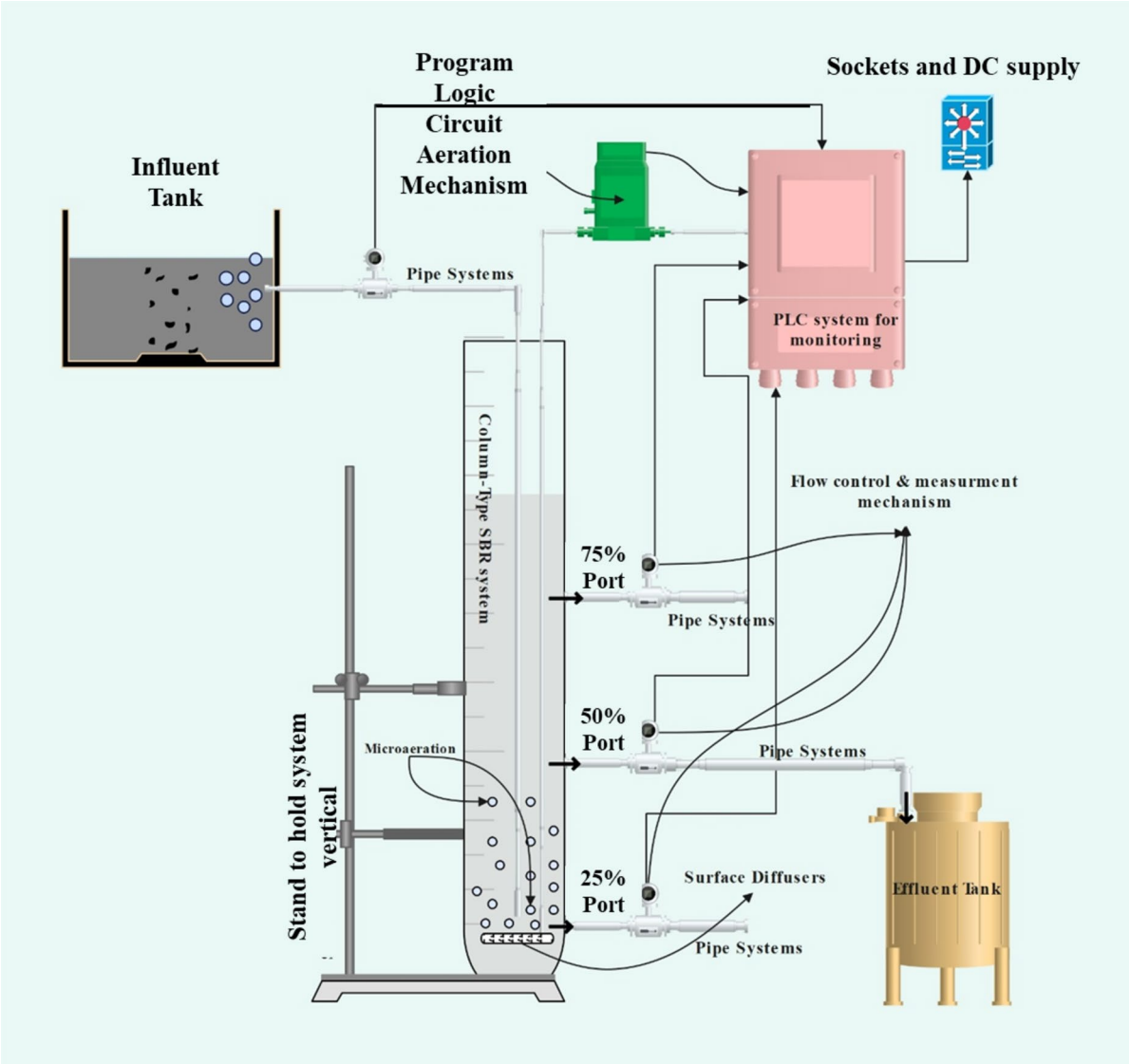

Fig. 2. Schematic diagram of experimental setup.

S. no	Nature of waste	Carbon to nitrogen ratio	Dissolved oxygen (mg/L)	Aerobic phase (hours)	Ammonia–nitrogen removal rate (mg /Lh)	References
1	Sewage	< 3–4	1	2.5	8.8	[35]
2	Sewage	< 3–4	0.5	3	7.3	[36]
3	Sewage	< 3	< 1	3	7.2	[37]
4	Sewage	< 3–3.5	< 1.5	3	9.3	[38]
5	Synthetic	3–17	3–4	1.33	9.6–12	[39]
6	Produced water	2–15	2–3	1	7–11	This study

Table 1. Aerobic and nitrogen removal studies.

The contributions of polyphosphate-accumulating organisms (PAO) and Glycogen Accumulating Organisms (GAO) to the intracellular carbon transformation are determined as follows:

$$COD_{heterogenous} = COD \times (1 - E_C) \tag{2}$$

$$COD_{\text{phosphate accumulating organism}} = \frac{PRA}{0.5 \times (COD_{in} - COD_{aer})} \tag{3}$$

Carbon to nitrogen ratio	Phase	The average value of total nitrogen in influent (mg/ L)	The average value of total nitrogen in effluent (mg/ L)	Total nitrogen removal (%)	Simultaneous nitrification denitrification (%)
2	Aerobic	25.2	20.3	20.3	14
6	Aerobic	12.5	10.3	13.6	15
10	Aerobic	12.4	3.2	74.6	78
15	Aerobic	12.5	2.4	67.4	65

Table 2. Total nitrogen in the cSBR at different C/N ratios.

$$COD_{\text{Glycogen accumulating organism}} = \frac{COD - COD_{OHO} - COD_{PAO}}{COD_{in} - COD_{aer}} \quad (4)$$

To establish the removal of TN in different phases of operation in cSBR using different nitrogen conditions, Ammonia–nitrogen, nitrate–nitrogen, and nitrite–nitrogen were analyzed to understand the SND process using Eq. 5.

$$SND = \frac{a_{in} - a_{eff}}{b_{in} - b_{eff}} \times 100\% \quad (5)$$

where a = TN (mg/L) is represented with subfix in-influent and eff-effluent during the different operation phases and b = ammonia–nitrogen.

Scheme of operation for sequencing batch reactors

The wastewater generated on the KFUPM campus at Dhahran University was used for treatment. A pilot scale column type cSBR was constructed using the Perspex material in all joints and sealed for any leakage. The Column-type reactor had a working volume of 3.31 liters and interior diameters of 75 mm. The column-type reactor has a height of 750 mm, as shown in Fig. 2. An air pump (EK8560, 6W) was used to maintain the aeration supply. The pump was coupled to the diffuser system at the reactor's bottom. This was carried out to ensure the DO content remained at 2–3 mg/L. The entire configuration was designed to function with a logic controlled by a programmed controller, i.e., a programmable logic controller system, in conjunction with solenoid and gate valves. The system was allowed to stabilize, after which experimental trials were carried out. At the beginning, the cycle period was established as 24 h and will progressively decrease to 6 hours by the conclusion of the trial. The influent port was made to connect with a solenoid valve with a sewage capacity of 12 liters. The solenoid valve is positioned at the topmost portion to allow it to work under gravity-driven flow. All the samples were collected at a port located at 50% of the tank's height, ensuring an equal volume interchange. Another port was located at a vertical position of 25% within the tank, specifically designed for sampling, collecting, and removing excess sludge. The sample and treatment procedures were conducted at ambient temperature. Table 3 illustrates the operational conditions of cSBR at different C/N ratios.

DNB sequencing

The collected samples from cSBR sludge were sent to Al Borg Diagnostics, Riyad, Saudi Arabia, for further analysis. The polymerase chain reaction was conducted by adding 30ng of DNA template and 16S rRNA (16S-V3-V4) fusion primers. The PCR products were purified using Agencourt AMPure XP beads, diluted in an Elution Buffer, and then labeled to form a library. The library's size and quantity were evaluated using the Agilent 2100 Bioanalyzer. Furthermore, specific libraries were subjected to sequencing using the DNB platform.

S. no	Parameters	Phase-I	Phase-II	Phase-III	Phase-IV	Phase-V	Phase-VI
	Period (days)	0–10	10–19	19–25	25–46	45–68	68–75
1	Cycle/eff. HRT (hr)	53	40	35	22	17	13
2	Chemical oxygen demand (mg/L) loading rate (kg COD/m^3/day)	0.32	0.44	0.55	1.63	2.5	4.5
3	NO_3^- (mg/L)	2.4	2.8	3.2	3.3	3.4	3.7
4	P–PO_4^{3-} (mg/L)	0.65	0.79	0.86	0.96	1.02	1.23
5	Sludge volume index (mL/g/MLSS)	90–110	102	112	61–70	60–89	74–80
6	Mixed liquor suspended solids (g/L)	2.0–3.0	3.0–3.1	3.1–3.2	3.2–3.3	3.3–3.4	3.4–3.5
7	Granule size (mm)	–	0.5–1.4	1.2–1.23	1.1–2.4	2.1–3.2	2.4–1.6
8	Integrity coeff. (%)	–	–	–	89	94	82

Table 3. Operational conditions of cSBR at different C/N ratios.

Bioinformatics analysis

Pre-processing of raw reads

Metagenomic raw data obtained are pre-processed to produce clean reads using the Fqtools module of iTools, check v.0.25, cutadapt v.2.6, and read v1.0. The raw reads are denoised by removing adapter and linker sequences, reads with a phred quality score of less than 25, low complexity reads, and reads with ambiguous base (N base). FLASH (Fast Length Adjustment of Short reads) v1.2.11 software was used to merge paired-end reads with a minimum overlapping length of 15 bp and the mismatching ratio of overlapped region < = 0.1 for connecting the Tags.

OTU clustering

Clustering the Tags into an Operational Taxonomic Unit (OTU) with a sequence similarity of 97% was conducted using the USEARCH v7.0.1090 software to obtain unique OTU representative sequences. Chimeras from the reads are checked and removed using UCHIME v4.2.40. The OTU abundance table was calculated by mapping tags to OTU representative sequences using USEARCH GLOBAL. The taxonomic annotation was generated by aligning OTU representative sequences against the Ribosomal Database Project database with a sequence identity cut-off of 60% using RDP classifier v2.2 software. OTU abundance table was utilized to perform OTU profile analysis and diversity analysis. The taxonomic annotation data were used to calculate species abundance in different levels of hierarchy consisting of Phylum, Class, Order, Family, Genus, and Species, and they were further used for functional annotation and species abundance analysis.

OTU profile analysis

The relative abundance of OTU in each sample is calculated in terms of bacteria, and the OTU rank curve was plotted, showing the abundance of the species according to rank in decreasing order using R v3.1.1 software.

Alpha diversity analysis

Alpha diversity analysis is carried out to evaluate the diversity of species in the sample. This was carried out by computing the Chao1 richness estimator (Chao1), abundance coverage-based estimator of species richness (ACE), Shannon–Weaver diversity index (Shannon), and Simpson diversity index (Simpson) using MOTHUR v.1.31.2 software.

Species abundance analysis

The GraPhlAn software was used to make a circular representation of multi-level species taxonomic classification of the microbial community within a sample. The phylogenetic tree of the species found in the sample was predicted using FastTree v2.1.3 package from R software using the maximum likelihood (ML) algorithm.

Functional annotation

The functional annotation of the microbial community of the sample was predicted based on marker gene sequence profiling from the 16S rRNA data using PICRUSt2 v2.3.0 software (Phylogenetic Investigation of Communities by Reconstruction of Unobserved States). The function prediction is based on the homology and assigning enzyme commission number. The metabolic pathway databases, including KEGG, MetaCyc, and COG (Clusters of orthologous groups of proteins), are utilized for studying metabolism at the subsystem level. The OTU taxonomic annotation data was used to categorize functional genes according to relative abundance at different levels. Further, the predictions are represented as histograms generated by R software.

ANN model development for prediction of COD removal and SND process prediction

Artificial neural network (ANN) modeling using MATLAB2016a was implemented to model the study and correlate the operational parameters with the COD and TN removal. TN removal indicates the simultaneous conversion of ammonia to nitrate by nitrification and then the conversion of the formed nitrate to nitrogen gas via denitrification. Out of all the operating parameters, aeration time, C/N ratio, and phosphate concentrations were found to profoundly impact COD and TN removal, as per various pieces of literature. The optimal C/N ratio for nitrogen and COD removal depends on the specific wastewater treatment process, the microbial community present, and the characteristics of the wastewater. Balancing the C/N ratio is crucial to ensuring efficient and effective removal of nitrogen and organic matter in wastewater treatment systems. Adjusting the C/N ratio by adding carbon or nitrogen sources can help optimize treatment performance based on the system's specific requirements[40]. Similarly, phosphate can enhance COD removal by providing extra carbon for microbial growth in some cases, but excessive levels can increase biomass production, potentially offsetting the benefits. Regarding TN removal, phosphate can compete with nitrate and nitrite, aiding in their reduction, yet high phosphate levels may interfere with phosphorus removal processes[40,41]. Hence, effective phosphate control is crucial to optimizing its wastewater treatment impact[42]. Found that intermittent aeration significantly improved TN and COD removal in an animal food plant wastewater treatment system. However[43], it was observed that high aeration rates led to sludge disintegration and poor COD removal efficiency using an SBR[44] demonstrated that continuous aeration enhanced COD removal but negatively affected nitrogen removal in aquaculture effluent treatment. Thus, aeration can positively affect COD and TN removal, but the specific impacts depend on the wastewater characteristics and treatment system design.

Based on the above literature survey, it was observed that aeration, $COD_{influent}/TN_{influent}$, and phosphorous had both positive and negative impacts on COD and TN removal. Hence, these three parameters were chosen as the input parameters, and COD and TN removal were selected as the target parameters for the ANN model.

The data from our study, comprising the input and output parameters, were stored in the workspace as two separate variables. The feedforward backpropagation technique was applied as the training function, and the Levenberg–Marquardt algorithm was chosen to train the data. The Levenberg–Marquardt algorithm was used to train the weights and biases of ANN because of its efficiency in optimizing the network's parameters. This algorithm combines gradient descent and Gauss–Newton methods, making it well-suited for nonlinear optimization problems like training ANN[45–47]. It adapts the learning rate during training, which helps it converge quickly while avoiding some of the pitfalls of other optimization algorithms. Its focus on minimizing the error between the predicted and actual outputs of the network makes it a popular choice for fine-tuning ANN parameters to improve model performance[47–49].

The number of neurons in the hidden layer varied from 5 to 20. The best network was chosen based on the high correlation coefficient (R) value and Mean squared error (MSE) values[47,50]. A sensitivity analysis of the best-fitted model was conducted to determine the relative influence of aeration time, C/N ratio, and phosphate concentrations on COD and TN removal. The process used for the sensitivity analysis has been described elsewhere[47,51]. Furthermore, the COD and TN removal efficiency was predicted for different data sets where experimentation was not carried out. This data set was used to study the interactive effect of any two parameters on COD and TN. The ANN can be regarded as a mathematical model. ANNs are a computational methodology that draws inspiration from the structure and functionality of biological neural networks in the human brain. These networks comprise interconnected nodes, sometimes known as neurons, arranged in layers. These layers include an input layer, one or more hidden layers, and an output layer. In addition, the ANN model was trained, tested, and verified using MATLAB during its development.

Furthermore, the objective of the ANN model was not to build a mathematical model but rather to enhance the operating conditions of the SND process to achieve optimal performance. The sensitivity analysis conducted using the ANN aimed to determine the parameter (C/N, phosphate, or aeration duration) significantly influenced COD and TN elimination. The ANN modeling involved varying the number of neurons from 5 to 20 and training the network to maximize the R and minimize the MSE values.

The maximum R-value and minimum MSE value were obtained when the number of neurons in the hidden layer was 10. Variations of R values with the change in the number of neurons in the hidden layer have been depicted in Fig. 3a and the optimized ANN architecture in Fig. 3b.

Results and discussion

Effects on the overall performance

Different characteristics like COD, BOD_5, and nutrients were characterized using different C/N ratios. The performance improves during the initial operation phases, and the system stabilizes. The values of COD were reported to increase initially and then started to fall as we went on increasing the C/N ratio, a maximum of 65.6% during 75 days of run. These contribute to the fact that external carbon sources can facilitate endogenous heterotrophs and organic degradation, but excess can reduce efficacy. It will also release secondary phosphorus in the anoxic phase. It is evident that as we increase the C/N ratio up to 10, the NH_4^+–N and TN removal increases, suggesting that the external carbon source enhances the SND process. The previous studies on sewage mainly focused on low carbon content and low DO to reduce the nutrients in the aerobic phase and help in endogenous denitrification. Autotropic denitrification primarily supplements with nitrifiers to achieve good efficacy. However, it is interesting to understand that low DO and slower nitrifier growth will result in lower nitrification. During this study, aeration was applied in a phased manner to enhance the development of nitrifiers; hence, higher C/N showed promising results and helped in the degradation of NH_4^+–N. The intracellular carbon transformation and nutrient removal were observed using control of phase manner operation parameters. In the aeration phase, a C/N ratio of 6 showed a high E_C of around 95% due to the leftover nitrates of the previous run. It may also be due to the fact that phosphate-accumulating organisms are the main reason for intracellular carbon transformation, using glycogen as an energy source and lowering the energy spent to convert external carbon into

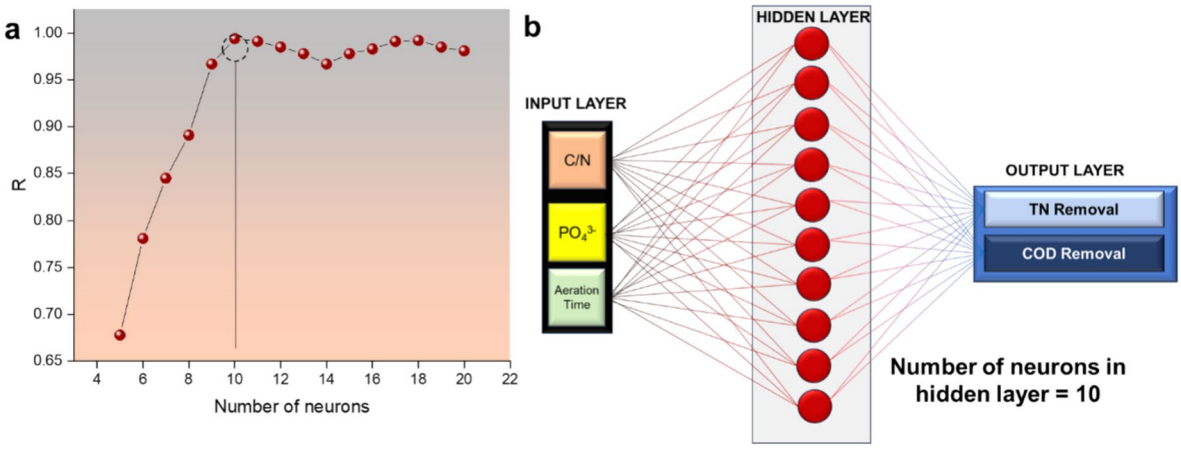

Fig. 3. (**a**) Variation of R values with the change in the number of neurons in the hidden layer, and (**b**) the architecture of the optimized neural network.

polyhydroxyalkanoates. Under different C/N ratio variations in the cSBR assisted with external carbon sources, it could enhance organic uptakes. Likewise, if C/N goes beyond 10, the hydrolysis becomes limited, and further increase will decrease the conversion of external carbon source. It is also essential to understand that conversion usually occurs in the aerobic phase and differs from the sewage treatment process.

The results show significant intracellular carbon conversion for absorption with the non-significant contribution of phosphate-accumulating organisms. The results also attributed that a higher C/N ratio can help enhance the denitrifying absorption. It is evident from Table 2 that a higher C/N ratio facilitated TN removal. It is a well-known fact that low C/N ratio often leads to scarcity of carbon with respect to nitrogen. As a result, nitrogen becomes the limiting factor, which in turn affects microbial activity, thereby decreasing COD and nitrogen removal[52,53.] However, at a higher C/N ratio of 15, there was a slight fall in TN removal. It is also essential to understand that increasing the C/N ratio will promote nitrification, which reverses the canonical theory of eutrophication for nitrification. As we go on, increasing the C/N ratio will help enrich heterotrophs and reduce the nitrifiers for ammonia and oxygen. The C/N ratio reaches 3, and the removal of TN in the anaerobic phase by an external carbon source shows a positive trend, enhancing denitrification. It is also essential to understand that when the C/N ratio reaches 10 in different stages of the aerobic cycle, it will be the main contributor to TN removal, thereby enhancing SND by 78%. The SND process considered by previous studies with a low C/N ratio showed low efficiencies attributed to ammonia assimilation under the low DO. Thus, indulgences of different phases, like anoxic and aerobic phases, for gradient DO will help in granule formation, which helps achieve a high rate of SND process overall. In the current study, we varied the external carbon source as a C/N ratio and found that organic carbon enhances the SND process until overdosing occurs. The higher SND process by autotrophic nitrifiers might be attributed to its inhibition and encourage nitrification at a high C/N ratio. The external carbon source enhances the SND process in different phases of cSBR operation, especially at C/N of 10, having an SND of around 78%. Microbial culture shows that C/N maintained at a certain level helps in intracellular carbon transformation and further enhancement in the SND process.

Effects of nitrite on the overall performance

After 75 days of operation, the pollutant removal efficiency varied under different anoxic nitrite concentrations in the cSBR system. The COD and nutrient removal in the various process phases were studied for 75 days. The results revealed that under different nitrite stresses, the C/N ratio and external carbon source had minimal effect on the TN removal. Also, the system's non-inhibitory nitrite at the start of each phase cycle shows high efficacy of phosphorus during 75 days of operation. But when the C/N ratio exceeds 10, the phosphorus reduces, i.e., the TP removal rate at 30 mg/L shows nitrite stress was about 69%. The variation observed during this study, like nitrite, increased the NH_4^+–N, thereby decreasing NO_3^-–N concentration, and hence an increase in NO_2–N was observed. They might be attributed to the non-inhibitory nitrite stress intensity, helping the SND process. It is also worth noting that high nitrite helps denitrification and dampens nitrification.

Effect of alkalinity and pH

The alkalinity and pH of the wastewater play a vital role in nitrification. Nitrifying bacteria, which are responsible for the conversion of ammonia to nitrate, are highly sensitive to pH, and they tend to work best when the pH ranges from 7 to 8[4]. During the nitrification process, H^+ ions are released, which tends to bring down the value of pH thereby making it acidic. At acidic pH conditions, the performance of the nitrifying bacteria is severely inhibited and affects the performance of the entire system. However, if there is sufficient alkalinity in the system, the change in pH is restricted. Hence, maintaining the alkalinity becomes crucial for the effective operation of the cSBR. The observed pH and alkalinity in the influent and effluent of cSBR over the entire period of operation have been shown in Fig. 4.

It was observed that the pH values dropped in the effluent for most of the cases. This may be attributed to the release of H^+ ions during nitrification[23,24,52]. However, in the initial phase and final stage of operation, there was an increase in pH. This might be because the production of oxidized pyridine nucleotides and ammonium during dissimilatory NO^{3-} reduction and respiratory denitrification raises the pH[54]. Furthermore, there is a possibility that the alkalinity of the effluent, which is an indication of its ability to neutralize acids, can also affect the pH oscillations that occur throughout the nitrification process. It is possible to achieve a rise in pH by counterbalancing the reduction in pH that is generated by nitrification. The typical values of stoichiometric conversion ratio of carbon to P-uptake were seen to lies in between 60:1 .This can be accomplished if the alkalinity concentration is sufficiently increased. On the other hand, there was a consistent drop of alkalinity in the effluent, which indicates the successful nitrification of ammonia, which in turn led to the formation of various organic acids[55]. The average value of alkalinity in the influent was 358 ± 16 mg/L as $CaCO_3$, and that in the effluent was 238 ± 31 mg/L as $CaCO_3$. The values indicate that there was sufficient alkalinity in the system to resist the fall in pH.

COD, nitrogen, and phosphorus metabolism potential under different C/N ratio

In SBR, the degradation of organic matter, quantified as COD, and the elimination of nitrogen and phosphorus largely depend on the metabolic functions of microorganisms in the activated sludge biomass. The C/N ratio in the influent wastewater is a crucial determinant that significantly impacts the various processes occurring within the conventional activated sludge process (ASP). Therefore, it is critical to investigate the impacts of different C/N ratios on these parameters[56,57].

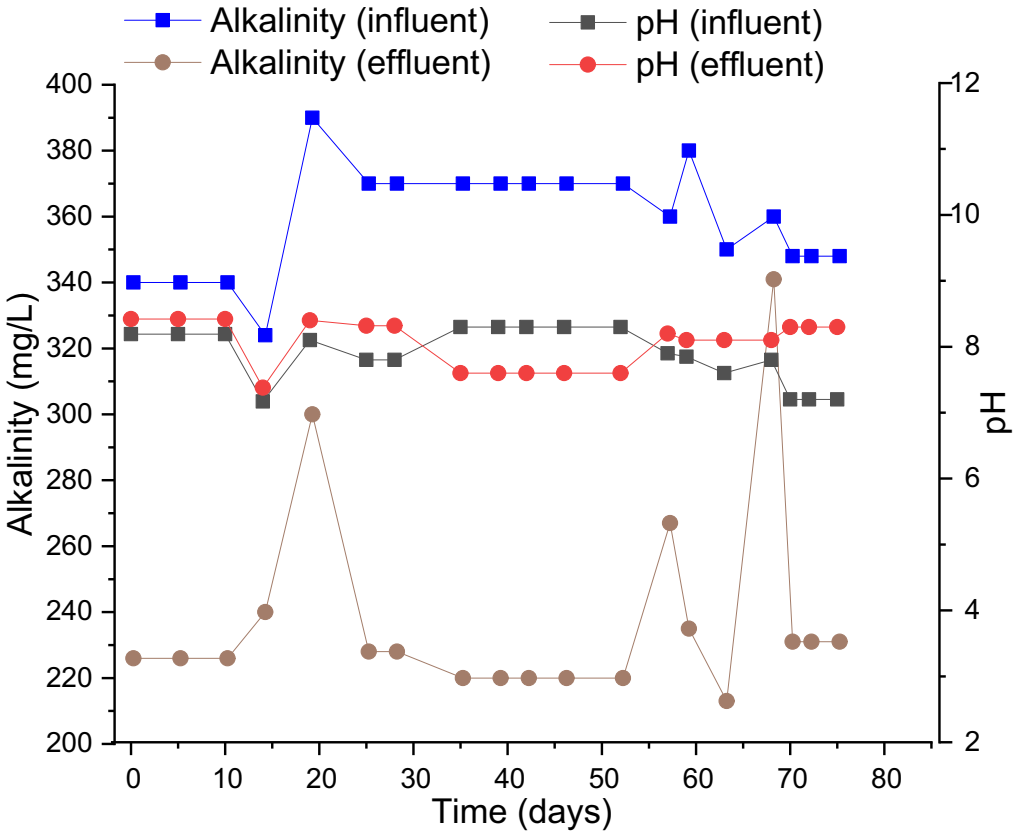

Fig. 4. Variation in alkalinity and pH in the influent and effluent of cSBR over the duration of operation.

COD metabolism

Microorganisms favor carbon over nitrogen utilization in wastewater with a high C/N ratio. This preference leads to the efficient removal of COD due to the higher carbon content in the wastewater. The surplus carbon is a source of energy and raw materials for the proliferation of heterotrophic bacteria responsible for degrading organic matter[40,58,59]. A low C/N ratio signifies an elevated nitrogen level compared to carbon within the incoming wastewater. In such cases, microorganisms may experience carbon limitation, resulting in reduced efficiency of COD removal. Optimizing the performance of the activated sludge process may require supplementary carbon sources or modifications to the C/N ratio[59,60].

Total nitrogen metabolism

Nitrification and denitrification mechanisms mainly facilitate the nitrogen removal process in an activated sludge system due to the high C/N ratio. An elevated C/N ratio fosters the process of nitrification, which involves the transformation of ammonium (NH_4^+) into nitrate (NO_3^-). Using carbon as an energy source is a crucial aspect of the nitrification process facilitated by nitrifying bacteria. The nitrification process can be carried out significantly efficiently, given the abundant carbon availability resulting from the elevated C/N ratio[40]. However, a reduced C/N ratio promotes denitrification, which converts nitrate to nitrogen gas (N_2), eliminating nitrogen. Nitrate serves as an electron acceptor for denitrifying bacteria when oxygen is restricted. In an environment with a low C/N ratio, the limited availability of carbon stimulates the process of denitrification[61]. However, in a system exhibiting a more excellent C/N ratio, a larger carbon pool can function as an organic carbon substrate for denitrifying microorganisms. The excess carbon in the environment aids denitrification by serving as a crucial source of energy and carbon substrate for the denitrifying bacteria. As a result, an increased C/N ratio has been observed to stimulate denitrification rates, ultimately resulting in enhanced TN elimination[40,62].

Phosphorus metabolism

The primary driver of biological phosphorus removal in an activated sludge process is the PAO, which is influenced by a high C/N ratio. In an environment with a high C/N ratio, PAOs exhibit efficient carbon uptake and intracellular storage as polyphosphate, thereby improving the removal of phosphorus from wastewater[40,63]. A reduced C/N ratio can hinder the capacity of PAOs to integrate carbon into polyphosphate synthesis, ultimately leading to decreased phosphorus removal effectiveness within the SBR. Optimal removal of phosphorus may require the inclusion of supplementary carbon sources or modifications to the C/N ratio[40,64,65]. It is crucial to consider that the efficacy of an activated sludge system (ASP) and the interplay among COD, nitrogen, and phosphorus elimination are impacted by multiple variables, such as temperature, hydraulic retention time, DO

concentrations, and the particular microbial community composition present in the activated sludge system. Thus, a holistic comprehension of these variables, combined with consistent surveillance and enhancement, is imperative to attain the intended results in wastewater treatment.

Understanding the role of phosphate, COD, and pH in the SND process.

Maintaining a balanced environment in microbial cultures is essential, especially in processes involving carbon and phosphorus metabolism, where nitrogen plays a critical role. Nitrogen is necessary for synthesizing proteins and nucleic acids, which are fundamental components of microbial cells. However, excessive nitrite concentrations can lead to toxicity in microbial cultures. High levels of nitrite can disrupt the microbial metabolism and impact cell viability. Nitrite toxicity can result in the dissociation of cell proteins because it can react with proteins, altering their structure and function. This can interfere with essential cellular processes and lead to cell damage or death. A high concentration of nitrite also dampens the electron transfer and substrate movement. Understanding stress conditions helps develop a model and the behavior of microbial cultures under toxic conditions and process efficiency. The microbial culture association, in either case, either increases or declines, which will help us predict the effluent COD removal efficiency and nutrient removal performances. It is also to understand that high nitrite stress intensity will favor denitrification and shorten the cycle of nitrification, which overall depends upon the bacterial community anyway. The nitrogen metabolic conversion pathway during the acceptance of electrons in biomass shows a decline in the NO_3 and NO_2^- and a rise in ammonia concentration. These results might be attributed to a decrease in microbial culture to convert ammonia to NO_2^- and NO_2^- to NO_3^-.

Prediction using ANN modeling, sensitivity analysis, and interactive effect study

The predicted vs. actual values of the optimized ANN network during the model's training, validation, and testing have been provided in Fig. 5a. The high R-value of 0.999 for training data sets, more than 0.98 for testing and validation data sets, and 0.994 for the complete dataset indicated that the model was a perfect fit. The MSE value for the complete dataset was also found to be as low as 6.84. It can be seen from Fig. 3a that the number of neurons in the hidden layer is 10, and the tansig function was used. The weights connecting the input layer neurons to the neurons in the hidden layer (IW) and weights connecting the neurons within the hidden or output layers (LW) have been provided in Table 4. The values of IW and LW in ANN are essential for the network's performance. These weights encode the knowledge and patterns learned from the training data, determining the strength of connections between neurons and shaping how information flows through the network. Input weights help the network assign significance to different input features, allowing it to focus on relevant information while filtering out noise. Layer weights within hidden layers enable the network to approximate complex, nonlinear functions and capture intricate relationships in the data. Properly tuned weights are crucial for the network's generalization to unseen data, its optimization during training, and its overall model performance.

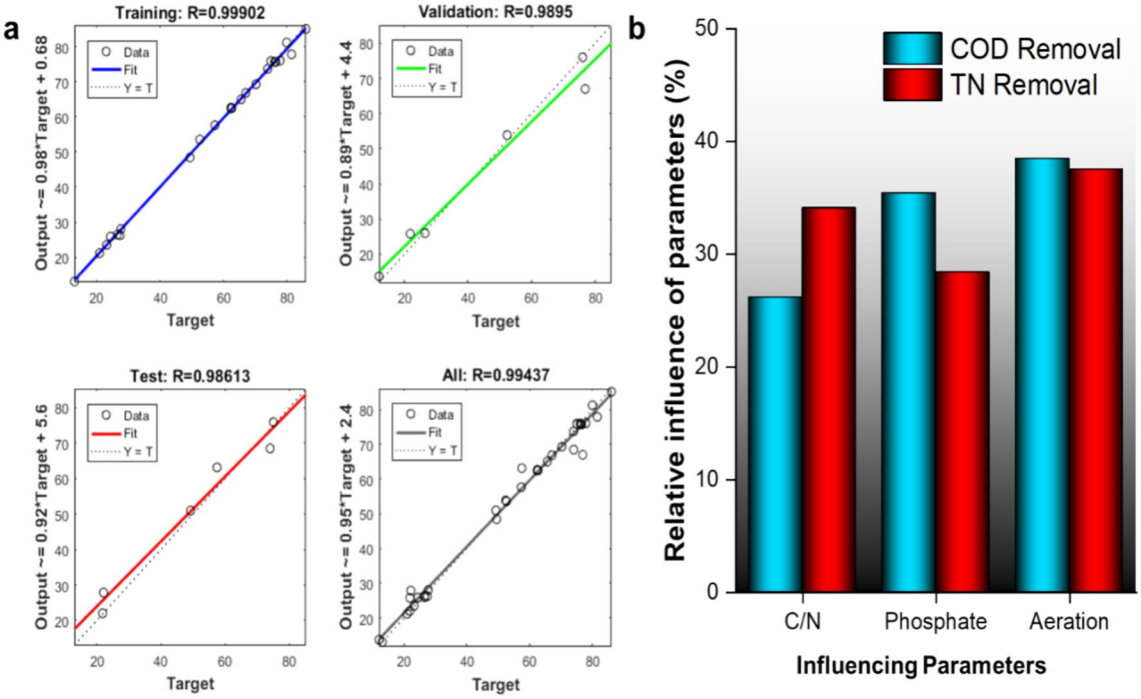

Fig. 5. (**a**) Fitting of training, validation, test, and all data sets vs the predicted data set obtained from the optimized artificial neural network model, and (**b**) influence of individual parameters on the removal of COD and TN.

Weights connecting the input layer neurons to the neurons in the hidden layer (IW)			Weights connecting neurons within the hidden or output layers (LW)	
−2.68252	0.751519	1.744131	−0.83958	0.78905
2.56534	−0.71827	2.266862	−0.41082	0.675335
1.808683	−2.4215	−1.23108	−1.49478	−1.01845
−2.15009	−0.12028	−2.85194	−0.30509	−1.7872
0.057387	−2.67363	−1.68768	1.126993	0.838934
−0.40719	−2.49671	2.867081	0.34737	−1.59513
0.264869	−0.88353	1.108538	−1.55332	−0.85437
−3.4714	−1.23674	−0.66028	−0.37147	2.027799
1.234707	0.679719	−2.0494	0.464208	0.046964
0.954095	1.76462	−2.31033	0.663435	0.499344

Table 4. Weights are obtained from the optimized artificial neural network model where the number of neurons in the hidden layer is 10.

The relative influence of aeration, phosphate, and $COD_{influent}/TN_{influent}$ ratio on COD and TN removal was obtained from sensitivity analysis. The results of the sensitivity analysis are shown in Fig. 5b. It was observed that the $COD_{influent}/TN_{influent}$ ratio had a more significant impact on TN removal, while phosphate had a more profound effect on COD removal. Aeration had the most significant impact and almost equally affected COD and TN removal.

The interactive effect of different operating parameters on COD and TN removal has been shown in Fig. 6. Contour plots illustrated the impact of varying two variables simultaneously on COD and TN removal efficiencies, revealing optimal conditions for the SND process in cSBRs. It was observed from Fig. 6a that a $COD_{influent}/TN_{influent}$ ratio of 5–8 favored COD removal. A higher $COD_{influent}/TN_{influent}$ ratio is associated with higher COD content. At an aeration time of 13.5 h, sufficient oxygen may not be available for the degradation of the excess COD[66]. Also, it was observed that there was an increase in COD removal with the increase in phosphate concentration. This is predominantly because phosphate availability can affect the growth and metabolism of microorganisms. Phosphate concentrations must be adequate for microbial energy production, enzyme synthesis, and cell growth. Low phosphate can inhibit microbial activity and reduce the efficiency of COD removal[67]. However, there was a drop in COD removal when the phosphate concentration was around 10–14. An increase in the $COD_{influent}/TN_{influent}$ ratio at low phosphate concentrations negatively affected TN removal (Fig. 6b). In the SND system, phosphorus availability is crucial in optimizing denitrification efficiency. Phosphate acts as a micronutrient and influences the activity of denitrifying bacteria. When phosphate concentrations are low, phosphorus can be limited, affecting the growth and activity of denitrifies[68]. As a result, denitrification may become less efficient, reducing TN removal.

Furthermore, the $COD_{influent}/TN_{influent}$ ratio and phosphate concentration can influence the microbial community structure in SND systems. Higher $COD_{influent}/TN_{influent}$ ratios and lower phosphate concentrations may favor the growth of heterotrophs or other less efficient microorganisms in denitrification[41]. These microorganisms may have different metabolic preferences or lower denitrification capabilities, ultimately impacting the TN removal efficiency. However, as phosphate concentration increased, TN removal increased. This is not only because phosphate favors microbial growth, but in the presence of high phosphate, there may be a prevalence of PAO, facilitating denitrification[40]. In Fig. 6c, it was observed that there was a decrease in COD removal with an increase in aeration time. In the SND process, low DO becomes the limiting factor for the nitrification of ammonia. However, when excess aeration is provided, and there is an abundance of DO, the growth of denitrifying bacteria gets affected. This results in low nitrate removal, thereby accumulating nitrate in the system. At the same time, the COD, which the denitrifying bacteria should utilize, also remains in the effluent. As a result, there was a decrease in COD removal and excess aeration[69]. In Fig. 6d, it was observed that the low $COD_{influent}/TN_{influent}$ ratio favored TN removal at low aeration, while at high aeration, the high CODinfluent/TNinfluent ratio favored TN removal. Usually, at a low $COD_{influent}/TN_{influent}$ ratio, nitrifying bacteria are dominant. Since down aeration time may lead to common DO conditions in the system, denitrifying bacteria may also be present.

As a result, high TN removal was observed at low $COD_{influent}/TN_{influent}$[40]. However, at high aeration times, COD may be degraded by heterotrophic bacteria, and there is less COD available for the complete denitrification of nitrates[40]. Hence, a high $COD_{influent}/TN_{influent}$ ratio is required. In Fig. 6e and f, the observation was that an increase in phosphate positively affected both COD and TN removal when the $COD_{influent}/TN_{influent}$ ratio was maintained at 7. This suggests that adding more phosphate to the system improved the removal of COD and TN when the $COD_{influent}/TN_{influent}$ ratio was kept at 7. A decrease in COD removal was observed in Fig. 6c, with an increase in aeration. However, TN removal increased with the rise in aeration (Fig. 6f). The COD may be due to the complete nitrification of ammonia during the aerobic phase[59].

The ANN model was further optimized to find the ideal condition for COD removal and TN removal and the optimum condition for simultaneous high COD and TN removal. It was found that maximum COD removal of 65.28% was predicted when the $COD_{influent}/TN_{influent}$ ratio was 9.5, phosphate concentration was 13 mg/L, and

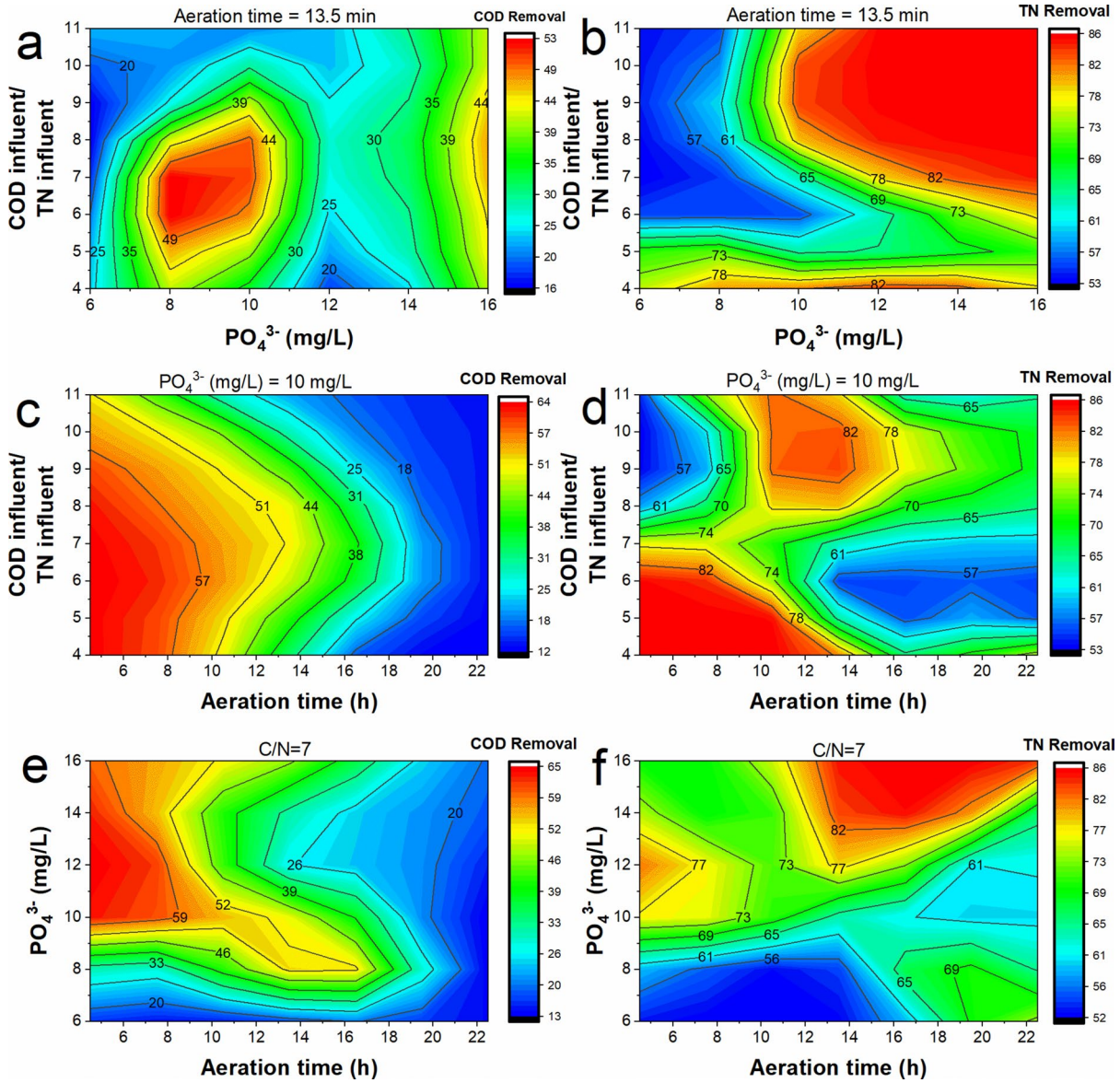

Fig. 6. Interactive effect of $COD_{influent}/TN_{influent}$ and phosphate on (**a**) COD and (**b**) TN removal, the interactive effect of $COD_{influent}/TN_{influent}$ and aeration time on (**a**) COD and (**b**) TN removal, and the interactive effect of aeration time and phosphate on (**a**) COD and (**b**) TN removal.

aeration time was 4.7 h. Similarly, the highest TN removal of 86.02% was expected to occur when the $COD_{influent}/TN_{influent}$ ratio was 4, phosphate concentration was 10.5 mg/L, and aeration time was 4.7 h. These findings are in line with the Fig. 6 and our earlier discussions. Consequently, the COD removal was also predicted to be around 63.7% at the abovementioned conditions. Furthermore, at this condition, optimum removal of COD (63.7%) and TN removal (86.02%) was also obtained. Hence, the optimum conditions for the current system's operation were predicted to be a $COD_{influent}/TN_{influent}$ ratio of 4, phosphate concentration of 10.5, and aeration time of 4.7 h.

Metagenomics study of sludge culture

The pre-processing of raw sequence from sequencing to produce clean data with 68,590 read pairs. After denoising and clustering the paired-end reads, 302 OTUs and 47,862 clean tags were obtained. The relative abundance of each OTU in the sample was computed. The OTU rank curve is shown in Fig. 7. The alpha diversity analysis was carried out to estimate the richness of species within a sample with the help of Chao1 (302), ACE (302), Shannon (3.241), and Simpson (0.096) indices. The estimated Chao1 and ACE indices were equal to the observed OTU number (Sobs = 302), and the Shannon and Simpson indices were low, implying that the diversity of the sample was low. The circular representation of the taxonomic classification in terms of phyla, order, and family of the microbial community present in the sample has been made using GraPhlAn software (Fig. 8). Pseudomonadota, Actinomycetota, and Bacteroidota were the top phylum present in the sample. Pseudomonadota (Proteobacteria) was the dominating phyla comprised of classes *Alphaproteobacteria, Betaproteobacteria,*

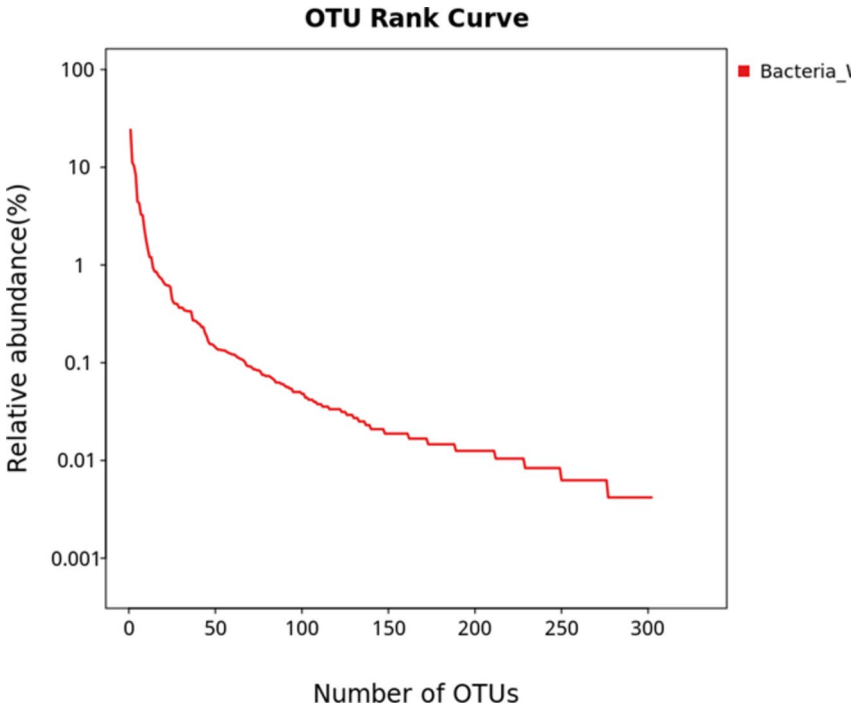

Fig. 7. Operational taxonomic unit (OUT) rank curve (relative abundance of each OTU in the sample).

and Gammaproteobacteria. To study the evolutionary relationship among the microbial community found in the sample, a phylogenetic tree was built using the maximum likelihood method (Fig. 9). The tree infers the neighboring clade of the Pseudomonadota is Bacillota (Firmicutes) and Chlamydia, which has a close relation with the phylum Verrumicrobiota. The relative abundance of functional genes was predicted from taxonomic annotated data associated with the metabolic pathway databases KEGG, MetaCyc, and COG using PICRUSt2 software. Based on the KEGG metabolic pathways, amino acid metabolism followed by carbohydrate and cofactor, vitamin metabolism showed more abundance (Fig. 10a). In the case of the COG database, amino transport and metabolism were predicted as the significant category followed by the genes involved in general function (Fig. 10b). Among the MetaCyc metabolic pathway prediction (Fig. 10c), even though function shown as Others with unknown function amino acid biosynthesis and biosynthesis of the cofactor, prosthetic groups, carrier, vitamin, and nucleotide and nucleoside biosynthesis formed the primary category (Fig. 7).

Future scope and prospective

The system described in this study could effectively remove TN through the SND process. The removal of COD was slightly on the lower side in the current system and further optimization studies was also be carried out to improve COD removal. Additionally, it is essential to evaluate the system's effectiveness in removing emerging contaminants and assess its performance in eliminating these substances. The system has the potential to treat wastewater containing high ammonia and phosphate. Domestic wastewater from households, agricultural wastewater from farming activities, and industrial wastewater from various industries (food processing, chemical manufacturing, and textile production are rich in ammonia and phosphates. Ammonia can come from organic waste decomposition and nitrogen-containing compounds, while phosphates often originate from detergents, fertilizers, and chemical discharges. These nutrients pose environmental risks if improper treatment leads to eutrophication and water quality degradation. Hence, implementing the current system for such wastewater treatment processes is crucial to mitigate the impact of high ammonia and phosphate levels and protect the receiving water bodies. The study shows that the system can effectively remove TN through SND in the presence of high phosphate and organic loading. Hence, this system can act as an innovative approach to treating domestic wastewater, agricultural run-off, and other industrial wastewater with high ammonia and phosphate loading. Furthermore, the C/N ratio had a more profound impact on TN removal than COD removal, while phosphate had a more profound effect on COD removal.

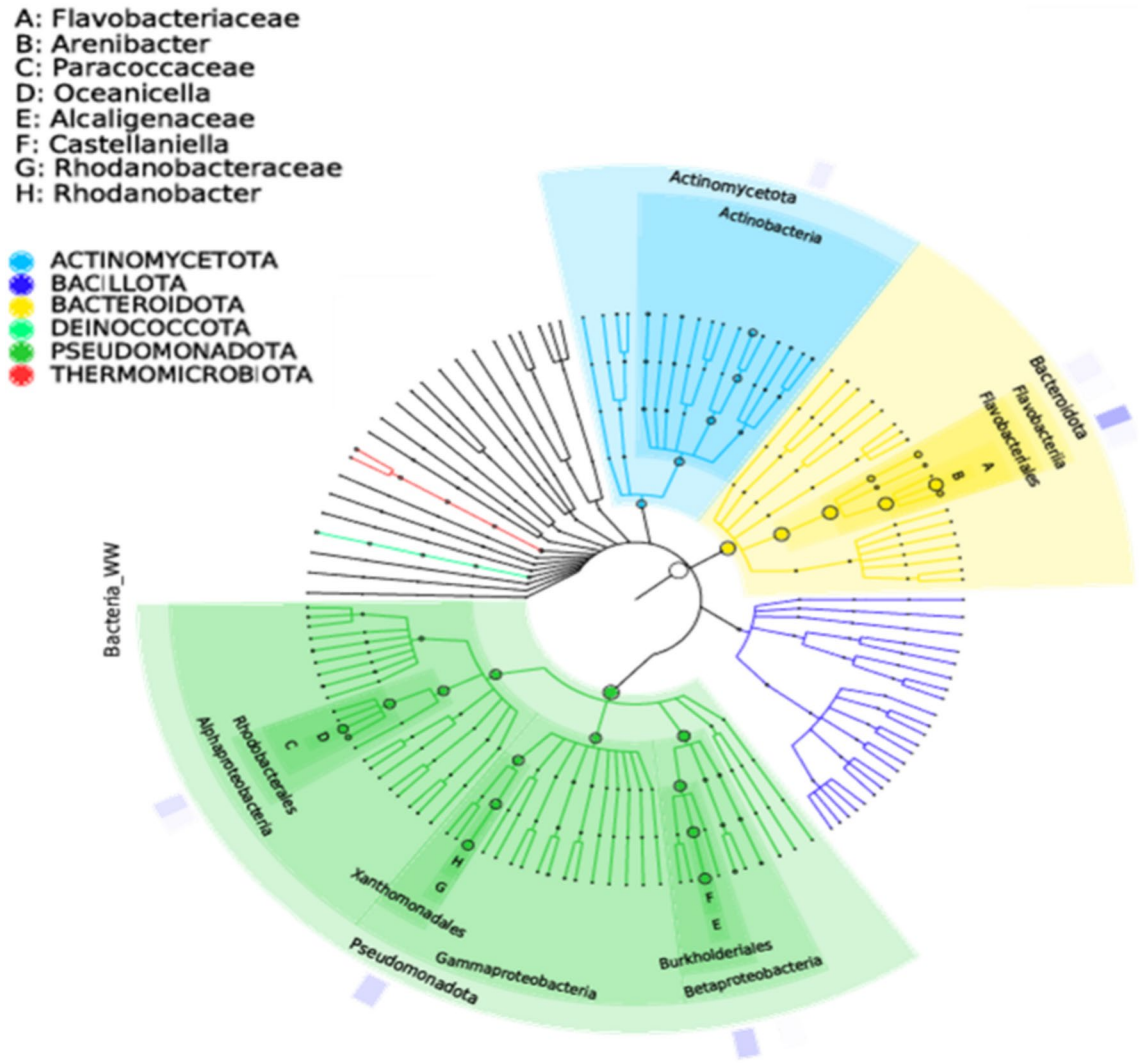

Fig. 8. Taxonomic classification in terms of phyla, order, and family of the microbial community representation.

Conclusion

To create a viable biological mechanism for SND in cSBR, the primary goal of this study is to analyze SND efficiency with variation in various operational parameters and to involve intracellular carob sources as functional genes throughout the SND process. Although the addition of external carbon sources often leads to increased operation and maintenance costs, excess sludge production, and chemical usage, it was observed that a higher C/N ratio could achieve better nitrogen removal. The findings suggested that improving the denitrifying metabolism may be facilitated by a greater C/N ratio. The external carbon source improves the SND process in all phases of cSBR operation at a C/N of 10, where SND is 78%. It is also essential to know that the aerobic cycle's C/N ratio is the main factor in nitrogen elimination and boosts SND by 78% when it reaches 10. The outcomes showed that phosphate-accumulating organisms did not considerably aid the primary intracellular carbon conversion for metabolism. Nonetheless, the results showed that a greater C/N ratio improves the denitrification process. After 75 days of operation, non-inhibitory nitrite at the start of each phase cycle increases phosphorus efficiency. When the C/N ratio is greater than 10, phosphorus decreases; the TP removal rate at 30 mg/L nitrite stress was 69%. Cell carbon conversion was found to be significantly affected by phosphate-accumulating organisms. Residual nitrates caused a 95% EC with a C/N ratio of 6. Higher C/N ratios improved nitrification and denitrification. However, a C/N ratio of 15 demonstrated a small negative effect on TN removal. These insights underscore the importance of optimizing the C/N ratio and phosphate concentration to enhance the performance of the SND process in wastewater treatment systems. Implementing this system could significantly mitigate the environmental impact of high ammonia and phosphate levels in various wastewater streams, including domestic, agricultural, and industrial sources.

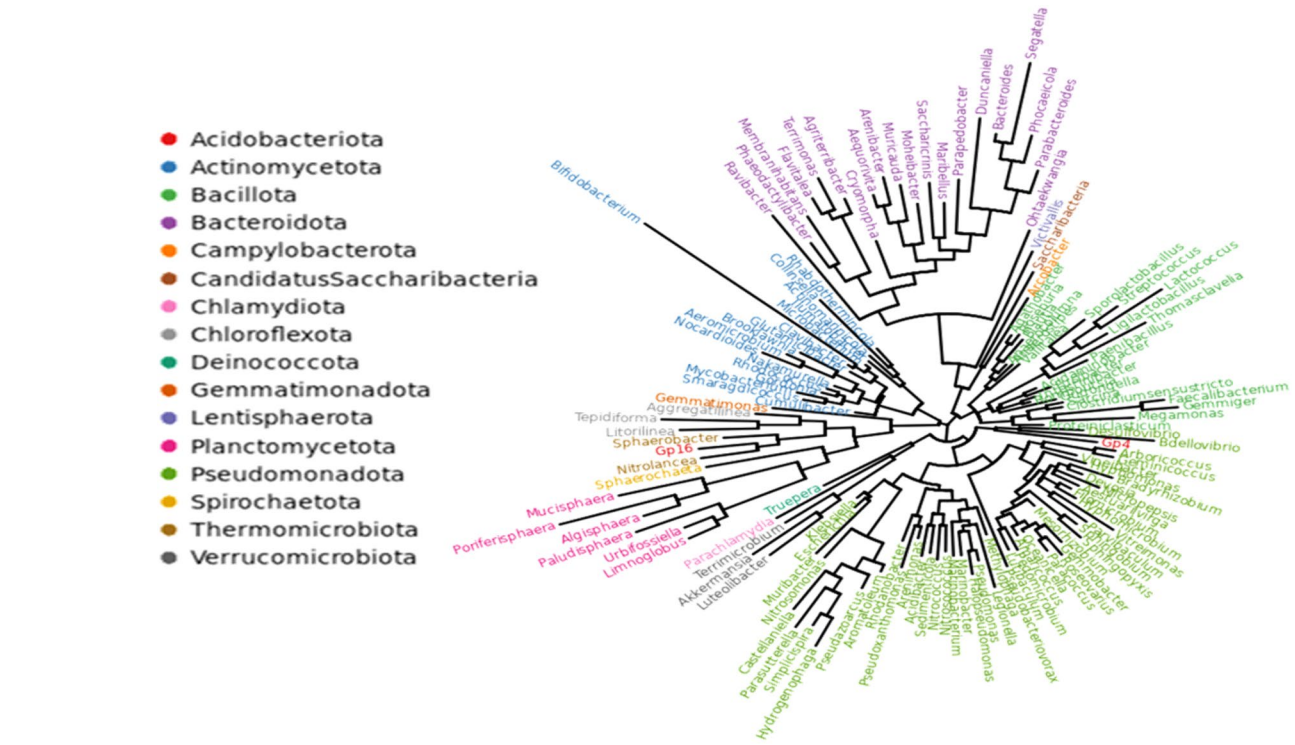

Fig. 9. Phylogenetic tree predicted using ML method by FastTree software.

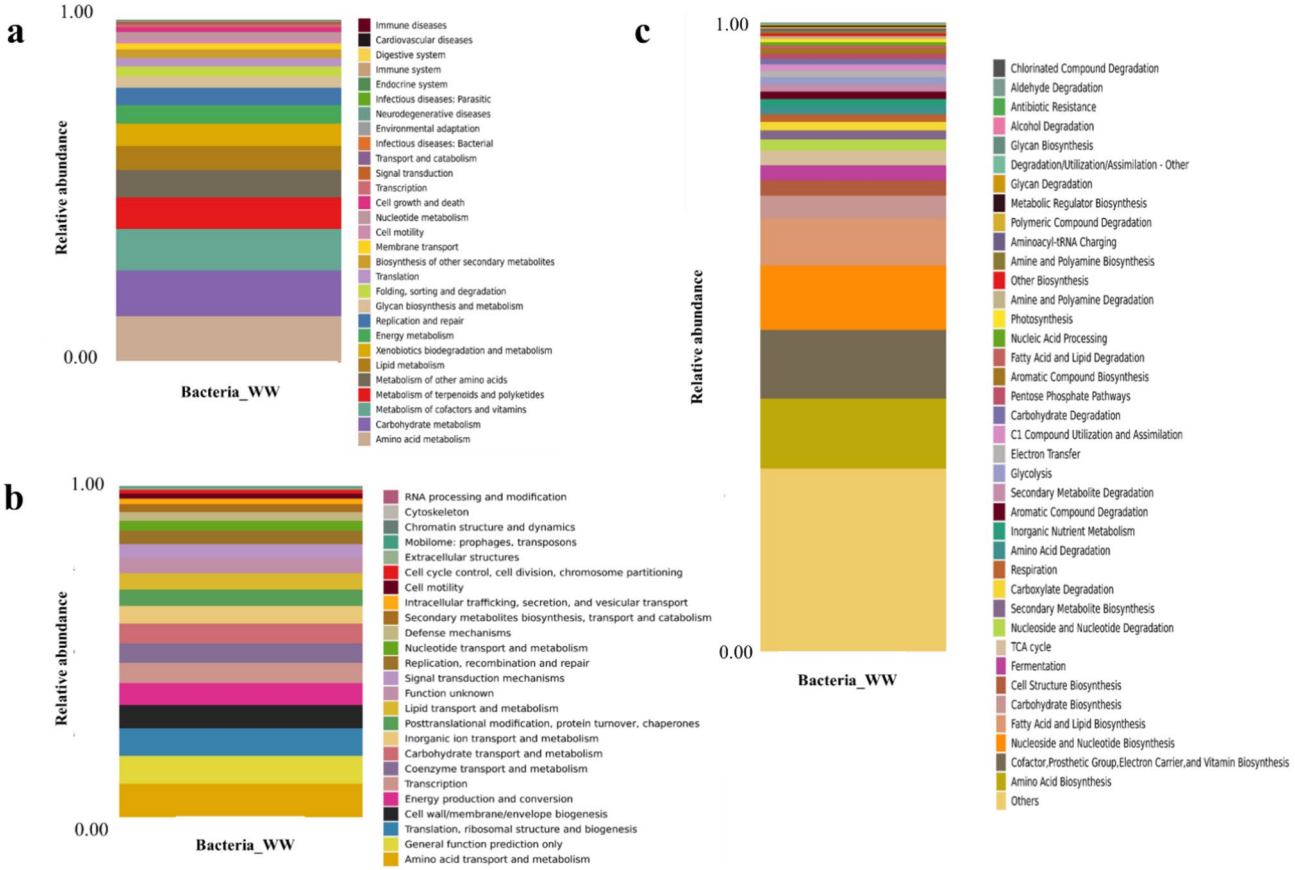

Fig. 10. The relative abundance of genes is categorized based on the subsystem in the metabolic pathways (**a**) KEGG database prediction, (**b**) COG database prediction, and (**c**) MetaCyc metabolic pathway prediction, inferring the majority of functional genes involved in amino acid biosynthesis, transport and biosynthesis of the cofactor, prosthetic groups, carrier, and vitamin and carbohydrate metabolism.

Data availability

The data that support the findings of this study are available from [Isam H Aljundi]. Still, restrictions apply to the availability of these data, which were used under license for the current study and are not publicly available. However, data are available from the authors upon reasonable request and with permission of [Isam H Aljundi].

Received: 23 June 2024; Accepted: 9 September 2024
Published online: 03 October 2024

References

1. Huang, S., Pooi, C. K., Shi, X., Varjani, S. & Ng, H. Y. Performance and process simulation of membrane bioreactor (MBR) treating petrochemical wastewater. *Sci. Total Environ.* **747**, 141311 (2020).
2. Soliman, M. & Eldyasti, A. Ammonia-oxidizing bacteria (AOB): opportunities and applications—a review. *Rev. Environ. Sci. Biotechnol.* **17**, 285–321 (2018).
3. Shukla, S., Rajta, A., Setia, H. & Bhatia, R. Simultaneous nitrification-denitrification by phosphate accumulating microorganisms. *World J. Microbiol. Biotechnol.* **36**, 151 (2020).
4. Jia, Y., Lv, S., Yang, T., Zhang, L. & Jiang, G. Effect of COD/NH4+-N and influent pH on the simultaneous nitrification and denitrification by using a sequencing batch reactor. in *2010 International Conference on Digital Manufacturing & Automation* vol. 1 604–607 (IEEE, 2010).
5. Biesterfeld, S., Farmer, G., Russell, P. & Figueroa, L. Effect of alkalinity type and concentration on nitrifying biofilm activity. *Water Environ. Res.* **75**, 196–204 (2003).
6. Liu, T., Li, Q., Wu, N. & Quan, X. Enhancing the formation of simultaneous nitrification and denitrification (SND) biofilm and nitrogen removal performance using two-units IFFAS process filled with surface-modified carriers. *Biochem. Eng. J* **179**, 108316 (2022).
7. Sandip, M. & Kalyanraman, V. Enhanced simultaneous nitri-denitrification in aerobic moving bed biofilm reactor containing polyurethane foam-based carrier media. *Water Sci. Technol.* **79**, 510–517 (2019).
8. Aghaei, A. *et al.* 14-Hybrid/integrated treatment technologies for oily wastewater treatment. In *Advanced Technologies in Wastewater Treatment* (eds Basile, A. *et al.*) 377–419 (Elsevier, The Netherlands, 2023). https://doi.org/10.1016/B978-0-323-99916-8.00002-X.
9. Haddaji, C. *et al.* Performance of simultaneous carbon, nitrogen, and phosphorus removal from vegetable oil refining wastewater in an aerobic-anoxic sequencing batch reactor (OA-SBR) system by alternating the cycle times. *Environ. Nanotechnol. Monit. Manag.* **20**, 100827 (2023).
10. Bahramian, M., Dereli, R. K., Zhao, W., Giberti, M. & Casey, E. Data to intelligence: The role of data-driven models in wastewater treatment. *Expert Syst. Appl.* **217**, 119453 (2023).
11. Yakamercan, E., Bhatt, P., Aygun, A., Adesope, A. W. & Simsek, H. Comprehensive understanding of electrochemical treatment systems combined with biological processes for wastewater remediation. *Environ. Pollut.* **330**, 121680 (2023).
12. Shi, S. *et al.* Overlooked pathways of endogenous simultaneous nitrification and denitrification in anaerobic/aerobic/anoxic sequencing batch reactors with organic supplementation. *Water Res.* **230**, 119493 (2023).
13. Cheng, Q., Chunhong, Z. & Qianglin, L. Development and application of random forest regression soft sensor model for treating domestic wastewater in a sequencing batch reactor. *Sci Rep.* **13**, 9149 (2023).
14. Noor, A. *et al.* Parametric optimization of additive manufactured biocarrier submerged in sequencing batch reactor for domestic wastewater treatment. *Heliyon* **9**, e14840 (2023).
15. Mehrani, M. J. *et al.* Application of a hybrid mechanistic/machine learning model for prediction of nitrous oxide (N_2O) production in a nitrifying sequencing batch reactor. *Process Saf. Environ. Prot* **162**, 1015–1024 (2022).
16. Wang, X. *et al.* Nitrite-resistance mechanisms on wastewater treatment in denitrifying phosphorus removal process revealed by machine learning, co-occurrence, and metagenomics analysis. *Environ. Pollut.* **327**, 121549 (2023).
17. Shi, S. *et al.* Overlooked pathways of endogenous simultaneous nitrification and denitrification in anaerobic/aerobic/anoxic sequencing batch reactors with organic supplementation. *Water Res.* **230**, 119493 (2023).
18. Mehrani, M. J. *et al.* Application of a hybrid mechanistic/machine learning model for prediction of nitrous oxide (N_2O) production in a nitrifying sequencing batch reactor. *Process Saf. Environ. Prot.* **162**, 1015–1024 (2022).
19. Uma, V. & Gandhimathi, R. Organic removal and synthesis of biopolymer from synthetic oily bilge water using the novel mixed bacterial consortium. *Bioresour. Technol.* **273**, 169–176 (2019).
20. Morgan-Sagastume, F. *et al.* Anaerobic treatment of oil-contaminated wastewater with methane production using anaerobic moving bed biofilm reactors. *Water Res.* **163**, 114851 (2019).
21. Miao, L. *et al.* Advanced nitrogen removal via nitrite using stored polymers in a modified sequencing batch reactor treating landfill leachate. *Bioresour. Technol.* **192**, 354–360 (2015).
22. Karschunke, K. & Sieker, C. Grenzen der Denitrifikation in der Biofiltrationstechnik am Beispiel der Kläranlage Nyborg. *Gas-und Wasserfach. Wasser, Abwasser* **138**, 337–344 (1997).
23. Pan, Z. *et al.* Effects of COD/TN ratio on nitrogen removal efficiency, microbial community for high saline wastewater treatment based on heterotrophic nitrification-aerobic denitrification process. *Bioresour. Technol.* **301**, 122726 (2020).
24. Fu, X. *et al.* Application of external carbon source in heterotrophic denitrification of domestic sewage: A review. *Sci. Total Environ.* **817**, 153061 (2022).
25. Zheng, B. *et al.* Effect of different C/N ratio on nitrogen removal of mariculture wastewater. *Res. Environ. Sci.* **33**, 1848–1856 (2020).
26. Chen, X. *et al.* Effect of C/N ratio on nitrogen removal of A/O-MBBR process for treating mariculture wastewater. *J. Ocean Univ. China* **20**, 879–885 (2021).
27. Dutta, A. & Sarkar, S. Sequencing batch reactor for wastewater treatment: recent advances. *Curr. Pollut. Rep.* **1**, 177–190 (2015).
28. Samocha, T. M. & Prangnell, D. I. Chapter 6-System Treatment and Preparation. In *Sustainable Biofloc Systems for Marine Shrimp* (ed. Samocha, T.M.B.T.-S.B.S.) 119–131 (Academic Press, Boca Raton, 2019). https://doi.org/10.1016/B978-0-12-818040-2.00006-X.
29. Ding, Y., Song, X., Wang, Y. & Yan, D. Effects of dissolved oxygen and influent COD/N ratios on nitrogen removal in horizontal subsurface flow constructed wetland. *Ecol. Eng.* **46**, 107–111 (2012).
30. Zhi, W. & Ji, G. Quantitative response relationships between nitrogen transformation rates and nitrogen functional genes in a tidal flow constructed wetland under C/N ratio constraints. *Water Res.* **64**, 32–41 (2014).
31. Zhang, C., Chen, H. & Xue, G. Coordination of elemental sulfur and organic carbon source stimulates simultaneous nitrification and denitrification toward low C/N ratio wastewater. *Bioresour. Technol.* **406**, 131069 (2024).
32. APHA & AWWA. *Standard Methods for Examination of Water and Wastewater. 22nd Ed. Washington: American Public Health Association*. *Standard Methods* (2012).
33. APHA & AWWA. *Standard Methods for Examination of Water and Wastewater. 22nd Ed. Washington: American Public Health Association*. *Standard Methods* (2012).
34. American Public Health Association. APHA Method 2550 Temperature: Standard Methods for the Examination of Water and Wastewater. *Standard Methods for the Examination of Water and Wastewater* 21, (2005).

35. Jin, Y. *et al.* Insight into the roles of microalgae on simultaneous nitrification and denitrification in microalgal-bacterial sequencing batch reactors: Nitrogen removal, extracellular polymeric substances, and microbial communities. *Bioresour. Technol.* **379**, 129038 (2023).
36. Ali, S. I., Moustafa, M. H., Nwery, M. S., Farahat, N. S. & Samhan, F. Evaluating the performance of sequential batch reactor (SBR & ASBR) wastewater treatment plants, case study. *Environ. Nanotechnol. Monit. Manag.* **18**, 100745 (2022).
37. Azeez, R. & Al-Zuhairi, F. Bio-treatment technologies of produced water: A review. *Eng. Technol. J.* **40**, 1–15 (2022).
38. Ali, S. I., Moustafa, M. H., Nwery, M. S., Farahat, N. S. & Samhan, F. Evaluating the performance of sequential batch reactor (SBR & ASBR) wastewater treatment plants, case study. *Environ. Nanotechnol. Monit. Manag.* **18**, 100745 (2022).
39. Azeez, R. & Al-Zuhairi, F. Bio-treatment technologies of produced water: A review. *Eng. Technol. J.* **40**, 1–15 (2022).
40. Saidulu, D., Srivastava, A. & Gupta, A. K. Elucidating the performance of integrated anoxic/oxic moving bed biofilm reactor: Assessment of organics and nutrients removal and optimization using feed forward back propagation neural network. *Bioresour. Technol.* **371**, 128641 (2023).
41. González-Tineo, P. *et al.* Organic matter removal in a simultaneous nitrification–denitrification process using fixed-film system. *Sci. Rep.* **12**, 1882 (2022).
42. Wosiack, P. A. *et al.* Removal of COD and nitrogen from animal food plant wastewater in an intermittently-aerated structured-bed reactor. *J. Environ. Manag.* **154**, 145–150 (2015).
43. Chang, G. F. *et al.* The effect of aeration rate on COD removal from high salinity wastewater in SBR process. *Appl. Mech. Mater.* **522**, 605–608 (2014).
44. Zhang, S., Li, G., Chang, J., Li, X. & Tao, L. Aerated enhanced treatment of aquaculture effluent by three-stage, subsurface-flow constructed wetlands under a high loading rate. *Pol. J. Environ. Stud.* **23**, 1821–1830 (2014).
45. Ghosal, P. S. & Gupta, A. K. Enhanced efficiency of ANN using non-linear regression for modeling adsorptive removal of fluoride by calcined Ca-Al-(NO3)-LDH. *J. Mol. Liq.* **222**, 564–570 (2016).
46. Yadav, M. K., Gupta, A. K., Ghosal, P. S. & Mukherjee, A. Modeling and analysis of adsorptive removal of arsenite by Mg–Fe–(CO3) layer double hydroxide with its application in real-life groundwater. *J. Environ. Sci. Health A Tox Hazard. Subst. Environ. Eng.* **54**, 1318–1336 (2019).
47. Majumder, A. & Gupta, A. K. Enhanced photocatalytic degradation of 17β-estradiol by polythiophene modified Al-doped ZnO: Optimization of synthesis parameters using multivariate optimization techniques. *J. Environ. Chem. Eng.* **8**, 104463 (2020).
48. Ghosal, P. S. & Gupta, A. K. Enhanced efficiency of ANN using non-linear regression for modeling adsorptive removal of fluoride by calcined Ca-Al-(NO3)-LDH. *J. Mol. Liq.* **222**, 564–570 (2016).
49. Yadav, M. K., Gupta, A. K., Ghosal, P. S. & Mukherjee, A. Modeling and analysis of adsorptive removal of arsenite by Mg–Fe–(CO3) layer double hydroxide with its application in real-life groundwater. *J. Environ. Sci. Health A Tox Hazard. Subst. Environ. Eng.* **54**, 1318–1336 (2019).
50. Majumder, A. & Gupta, A. K. Kinetic modeling of the photocatalytic degradation of 17-β estradiol using polythiophene modified Al-doped ZnO: Influence of operating parameters, interfering ions, and estimation of the degradation pathways. *J. Environ. Chem. Eng.* **9**, 106496 (2021).
51. Majumder, A. & Gupta, A. K. Kinetic modeling of the photocatalytic degradation of 17-β estradiol using polythiophene modified Al-doped ZnO: Influence of operating parameters, interfering ions, and estimation of the degradation pathways. *J. Environ. Chem. Eng.* **9**, 106496 (2021).
52. Tchobanoglous, G., Stensel, H. D., Tsuchihashi, R. & Burton, F. Metcalf and Eddy, AECOM - Wastewater Engineering: Treatment and Resource. 2048 Preprint at (2013).
53. Kamilya, T., Majumder, A., Saidulu, D., Tripathy, S. & Gupta, A. K. Optimization of a continuous hybrid moving bed biofilm reactor and constructed wetland system for the treatment of paracetamol-spiked domestic wastewater. *Chem. Eng. J.* **477**, 147139 (2023).
54. Rust, C. M., Aelion, C. M. & Flora, J. R. V. Control of pH during denitrification in subsurface sediment microcosms using encapsulated phosphate buffer. *Water Res.* **34**, 1447–1454 (2000).
55. Kendall, C., Doctor, D. H. & Young, M. B. 79 - Environmental Isotope Applications in Hydrologic Studies. In *Treatise on Geochemistry* (eds Holland, H. D. & Turekian, K. K.) 273–327 (Elsevier, Oxford, 2014). https://doi.org/10.1016/B978-0-08-095975-7.00510-6.
56. Kanders, L., Yang, J. J., Baresel, C. & Zambrano, J. Full-scale comparison of N2O emissions from SBR N/DN operation versus one-stage deammonification MBBR treating reject water – and optimization with pH set-point. *Water Sci. Technol.* **79**, 1616–1625 (2019).
57. Fontenot, Q., Bonvillain, C., Kilgen, M. & Boopathy, R. Effects of temperature, salinity, and carbon: nitrogen ratio on sequencing batch reactor treating shrimp aquaculture wastewater. *Bioresour. Technol.* **98**, 1700–1703 (2007).
58. Saidulu, D., Srivastava, A. & Gupta, A. K. Elucidating the performance of integrated anoxic/oxic moving bed biofilm reactor: Assessment of organics and nutrients removal and optimization using feed forward back propagation neural network. *Bioresour. Technol.* **371**, 128641 (2023).
59. Tchobanoglous, G., Burton, F. L. & Stensel, H. D. *Wastewater Engineering: Treatment and Resource Recovery* (Metcalf & Eddy Inc. McGraw-Hill Education, Boston, 2014).
60. Zhou, Z., Qi, M. & Wang, H. Achieving partial nitrification via intermittent aeration in SBR and short-term effects of different C/N ratios on reactor performance and microbial community structure. *Water (Basel)* **12**, 3485 (2020).
61. Sun, Q. & Zhu, G. Simultaneous denitrification and antibiotic degradation of low-C/N-ratio wastewater by a three-dimensional biofilm-electrode reactor: Performance and microbial response. *Environ. Res.* **210**, 112856 (2022).
62. Kocaturk, I. & Erguder, T. H. Influent COD/TAN ratio affects the carbon and nitrogen removal efficiency and stability of aerobic granules. *Ecol. Eng.* **90**, 12–24 (2016).
63. Wang, Q. *et al.* Phosphorus removal performance of microbial-enhanced constructed wetlands that treat saline wastewater. *J. Clean. Prod.* **288**, 125119 (2021).
64. Kamilya, T. *et al.* Nutrient pollution and its remediation using constructed wetlands: Insights into removal and recovery mechanisms, modifications and sustainable aspects. *J. Environ. Chem. Eng.* **10**, 107444 (2022).
65. Wang, Q. *et al.* Phosphorus removal performance of microbial-enhanced constructed wetlands that treat saline wastewater. *J. Clean. Prod.* **288**, 125119 (2021).
66. Yu, G. *et al.* Enhanced nitrogen removal of low C/N wastewater in constructed wetlands with co-immobilizing solid carbon source and denitrifying bacteria. *Bioresour. Technol.* **280**, 337–344 (2019).
67. Bergwitz, C. & Jüppner, H. Phosphate sensing. *Adv. Chronic Kidney Dis.* **18**, 132–144 (2011).
68. Bergwitz, C. & Jüppner, H. Phosphate sensing. *Adv. Chronic Kidney Dis.* **18**, 132–144 (2011).
69. Rong, Q. I., Kun, Y. & Yu, Z. Treatment of coke plant wastewater by SND fixed biofilm hybrid system. *J. Environ. Sci.* **19**, 153–159 (2007).

Acknowledgements

The authors express their gratitude to the Interdisciplinary Research Center for Membranes and Water Security (IRC-MWS) and King Fahd University of Petroleum and Minerals, Dhahran, Saudi Arabia, for their support in

the current research. Simranjeet would like to thank DBT RA (DBT-RA/2022/July/N/2044) and MoE-STARS/STARS-2/2023-0714.

Author contributions

N.A.K., A.M., S.S, P.C.R and I.H.A.: Conceptualization, Data curation, Formal analysis, Investigation, Methodology, Visualization; Writing an original draft, Writing—review & editing. N.A.K., A.M., S.S., N.M., P.C.R., D.L., I.H.F: Data curation, Formal analysis, Investigation, Methodology, Visualisation, Validation, D.L: Setup fabrication, Supervision, review & editing, I.H.A.: Resources, Project guidance, Supervision, Validation. Writing, review & editing. I.H.A., P.C.R and I.H.F: writing, review and final editing the manuscript.

Funding

This research did not get any dedicated support from public, commercial, or not-for-profit organizations.

Competing interests

The authors declare no competing interests.

Additional information

Correspondence and requests for materials should be addressed to N.A.K. or I.H.A.